Universitat Politècnica de Catalunya (UPC)
Universitat Autònoma de Barcelona (UAB)
Universitat de Barcelona (UB)
Institut de Ciències Fotòniques (ICFO)

http://www.photonicsbcn.eu

Master in Photonics

MASTER THESIS WORK

3D OPTICAL MICROSCOPY FOR "EX-VIVO" WHOLE BRAIN IMAGING

Angela Vazquez Quintian

Supervised by Dr. Ivan Amat-Roldan, (IDIBAPS, UB)
Dr. David Artigas Garcia (UPC)

Presented on date 9th September 2010

Registered at

Escola Tècnica Superior d'Enginyeria de Telecomunicació de Barcelona

3D Optical microscopy for “ex-vivo” whole brain imaging

Angela Vazquez Quintian
Institut d'Investigacions Biomèdiques August Pi i Sunyer (IDIBAPS), Hospital Clinic, Universitat de Barcelona, Villarroel 170, Barcelona 08036, Spain

E-mail: avazq1331@upc.edu

Abstract. The work presented in this paper focuses in understanding a light sheet microscope. Light sheet microscopy consists in a thin sheet of light which illuminates the observed sample in the plane orthogonal to the objective, thus allowing the observation of the internal structure. In this work we particularly focus in the impact of one of the main elements of such microscope: the slit. Optimizing different optical elements of a light sheet microscope to obtain images of cleared samples of animal brains about 2cm of diameter. This will allow obtaining microscopic images of organs in the centimetre range. In the optimization of a light sheet microscope several parameters are critical, like the slit aperture, the laser waist and the focal distance to the tube lens. Future developments of this setup will allow obtaining 3D reconstruction of interior structures, avoiding histological slicing of the specimens. The applications of this kind of microscopy in life sciences are numerous.

Keywords: light sheet microscopy, optical sectioning, optical tissue clearing, 3D scanning

1. Introduction

During the last century the increasing interest in health and welfare has heightened the study of new imaging technologies for scientific applications such as microbiology or medical diagnosis. In this research area two branches are clearly differentiated: macroscopic scale and microscopy scale. In the first field widely used techniques are Computer Tomography (CT), Magnetic Resonance Imaging (MRI) and Positron Emission Tomography (PET). All of them are suitable for whole macroscopic object imaging. However, the resolution achieved does not resolve individual cells. Related to microscopic scale, confocal microscopy and 2-photon microscopy present limited penetration depths, because they cannot use low numerical aperture (NA) objectives that provide large depth of field.

Nowadays, the highest resolution for sample size of the order of centimetres is attained by using histological sectioning. Nevertheless, 3D reconstruction is a laborious process with inaccurate results due mainly to misalignments and distortions that are inevitable during the slicing procedure [1]-[2].

The purpose of this investigation was to study an alternative to histological slicing, based in optical sectioning of whole objects. To achieve an optical section a thin sheet of laser light illuminates the sample in the focal plane of the objective to avoid the generation of stray-light and image blurring. Furthermore, this light should be able to go through the object to visualize the entire plane of the organ, and this just can be attained by using non-opaque samples. Therefore, in this approach two techniques are combined: ultramicroscopy to generate the light sheet, and optical clearing of the sample. Thus, imaging of macroscopic objects could be possible with microscopic resolution.

Light sheet microscopy was developed 100 years ago by Richard Adolf Zsigmondy (1865 - 1929), who was awarded a Nobel Prize in 1925 for his research on colloids and the ultramicroscope [3].

The initial ultramicroscope was adapted in this research to obtain the single optical sections. Briefly, the sheet of light is formed expanding the gaussian laser beam using a beam expander. The light passes through a slit aperture of diameter 1 mm and is focused by a cylindrical lens to shape the light sheet. In contrast to confocal microscopy, illumination and observation pathways are separated, and thus also low NA objectives can be used.

The optical clearing process is an idea exploited over decades in biology. The principle of tissue clearing is based in the previous dehydration of the sample, and after that, the immersion of the organ with a substance which has the same refractive index as proteins [4]. As a result, when tissue is completely infiltrated with the clearing agent, it becomes translucent reducing the light scattering, and thus, allowing the delivery of light deeper in the sample.

The remainder of this paper is divided into four sections. First, the methodology applied during this experiment is detailed. Second, the results obtained are shown. Third, a discussion of the results is presented. Finally, the conclusions derived from this work are summarized.

2. Methods

2.1. Preparation of the samples: tissue clearing

The biologists working at *Fetal and Perinatal Medicine Research Group (IDIBAPS)* are in charge of preparing the samples from experimental rabbits. The samples employed in this investigation were neonatal rabbit brains and hearts, 30 days of gestation and were prepared according to the research group methods.

The samples employed in this investigation were neonatal rabbit brains and hearts, 30 days of gestation. After the rabbit was killed, the organs were extirpated and placed in 4% paraformaldehyde in 0.1 M Phosphate Buffering Saline (PBS) for 1 week at 4ºC. PBS is a buffer solution commonly used in biological research. It is a water-based salt solution containing sodium chloride, sodium phosphate, potassium chloride and potassium phosphate. The buffer helps to maintain a constant pH. Then, the tissue was dehydrated in a graded ethanol series, ranging from 30º to 100º at room temperature, one day each component. The organs were rinsed in >99% Hexane for one hour at room temperature in order to achieve maximal dehydration. Afterwards, these were transferred into the clearing solution in a proportion 1:2 (Benzyl alcohol: Benzyl benzoate), n=1.56 [5]. Eventually, the samples were stored in the clearing solution for at least two days at room temperature before imaging.

Figure 1 shows the transparent brain of neonatal rabbit when it is illuminated with the light sheet. The size of this organ is approximately 4x2.5x2 cm. Here, the brain is in the clearing solution and the light sheet from the cylindrical lens goes through the sample. The first image is useful to evaluate the high level of transparency achieved. Although in figure 1.b the brain is invisible, it’s seen how the light goes through it, right behind the centre of the objective.

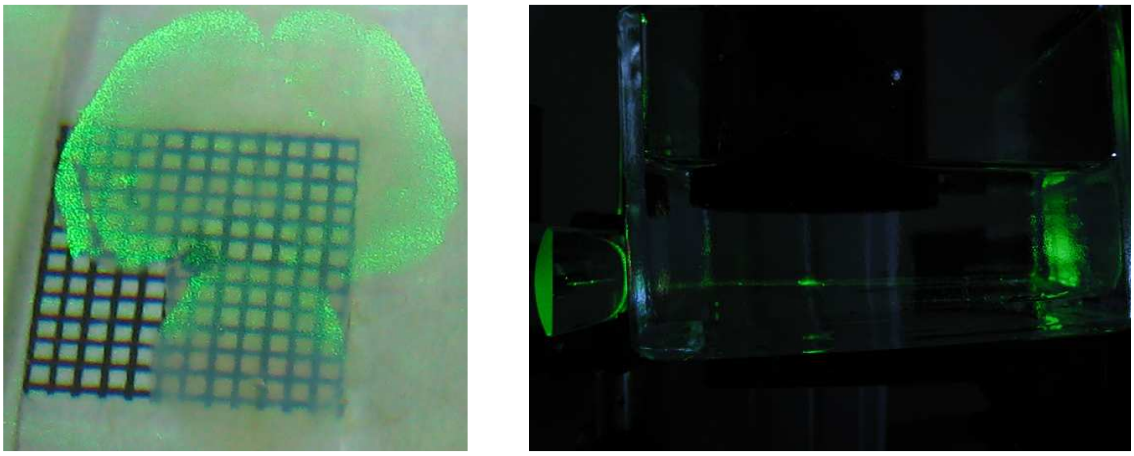

(a) (b)

Figure 1.Optical section in a transparent sample: (a) view from the top, (b) lateral view.

2.2. Ultramicroscope: experimental setup

The ultramicroscope built for this experiment was composed of the illumination part, that forms the planar light sheet, and the imaging train, where the CCD camera captures the illuminated 2D section of the sample. Figure 2 presents the whole setup in which the laser beam goes through the optical elements to the 3D stage, monitorized by the computer, as well as the camera.

The light source was a diode-pumped solid state green crystal laser (CristaLaser, coherent, λ=561 nm, CW). The output power was 50 mW, intense enough to burn a small sample over long-term exposure. The laser beam was attenuated by using a 3 dB attenuator, so the actual power employed in the setup was 25 mW. In this class III-B laser this power level is still critical, wearing goggles was required (labelled LG10) to prevent retinal hazard. The laser beam was reflected in four 45º mirrors, and went through two pinholes to verify the alignment of the beam before entering the microscope. The beam expander was based in Galilean telescope. This consisted in two plano-convex lenses that expanded the beam by a factor M (magnification), following (1) [6]:

$$M = \frac{f_2}{f_1} = \frac{D_1}{D_2} \tag{1}$$

Where f_1=30 mm and f_2=250 mm are the focal lengths of the first and second lenses in figure 2, D_1 and D_2 their respective diameters. Since the distance between both lenses is $d_{exp}=f_1+f_2$ (focused), they were chosen to fit in the setup but also to fulfill the required beam magnification. Therefore, the separation between both lenses was d_{exp}=280 mm and the total magnification M=8.33. This means that the laser beam with diameter equal to 2.50 mm, after the last mirror, became 20.83 mm at the output of the expander.

The cylindrical lens has curvature in one dimension (it can perform a 1D Fourier transform), so focuses light in one dimension only. Thus, this lens transforms a collimated circular gaussian beam of light into an elliptical gaussian beam with high eccentricity (almost line image). In this setup was used a cylindrical lens which focal length was 50 mm.

The next step was to choose the adequate slit aperture. This element was fundamental to shape the light sheet, since its lateral width depends inversely on the slit’s diameter, as shown in (2)-(5). As the laser beam is Gaussian, the beam width varies along the direction of propagation. The full angle of beam divergence, it is the cone angle of the asymptote to the beam profile at the beam waist ($2w_0$), is [7]:

$$\theta \approx \frac{\lambda}{\pi w_0} \tag{2}$$

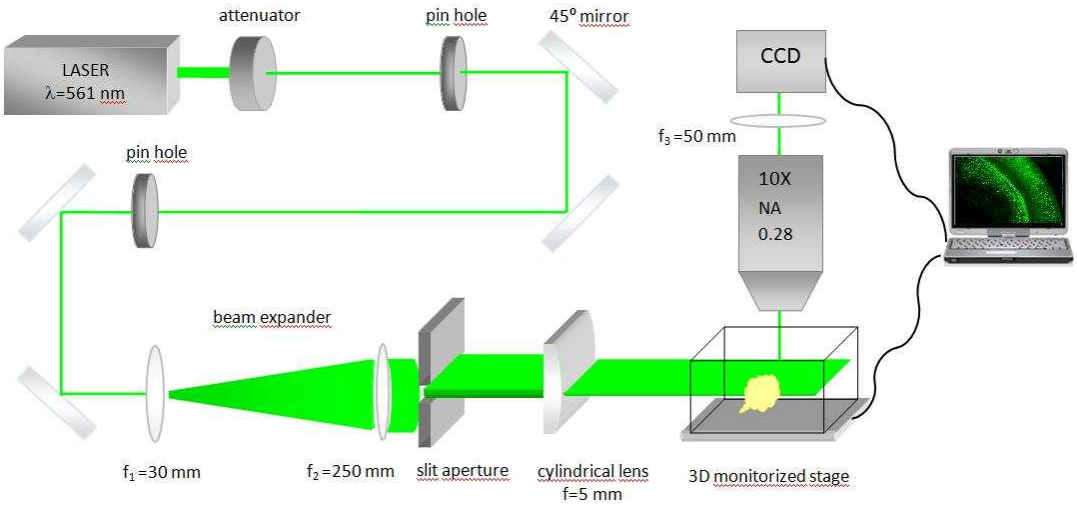

Figure 2.Ultramicroscope setup.

Since angle θ approximately is *w/f* , the minimum beam width w_0 is:

$$w_0 = \frac{\lambda f}{\pi w} \tag{3}$$

Where w_0 denotes half of the minimal light sheet width (half beam waist), w half of the diameter of the slit aperture and f the focal length of the cylinder lens, being $f = 50\ mm$ in this setup, and λ=561 nm, the laser wavelength.
The variation of the beam diameter at distance *z* is defined by the $1/e^2$ cutoff points (13.5% of the peak) of the Gaussian beam profile, and is given by (4):

$$w^2(z) = w_0^2 + \theta^2 z^2 \tag{4}$$

Thus, the width of the light sheet in any point *z* in the direction of propagation is:

$$w(z) = w_0\sqrt{1 + \left(\frac{\lambda z}{\pi w_0^2}\right)^2} \tag{5}$$

Figure 3 shows the lateral beam shape for three different slit apertures dimensions (w= 0.5 mm, w=1 mm and w=2 mm). In conclusion, a smaller beam waist in the centre means a larger beam width at a distance z. And both thickness, w_0 and $w(z)$, depend on the slit aperture. Therefore, it is a good compromise to use a slit width that results in a light sheet thickness at the sides of the specimen of $\sqrt{2}w_0$ [8], this is:

$$\left(\frac{\lambda z}{\pi w_0^2}\right)^2 = 1 \tag{6}$$

Then, by substituting (3) in (6):

$$w(z) = \sqrt{\frac{\lambda f^2}{\pi z}} \tag{7}$$

In this experiment, the length of the brain used was approximately 20 mm, that is z=10 mm. Therefore, the diameter of the slit aperture (d=2w) that fulfills with above mentioned criteria is d=0.4 mm. However, due to mechanical issues the minimal slit obtained was d=1 mm, which shape is illustrated in figure 3 (blue).

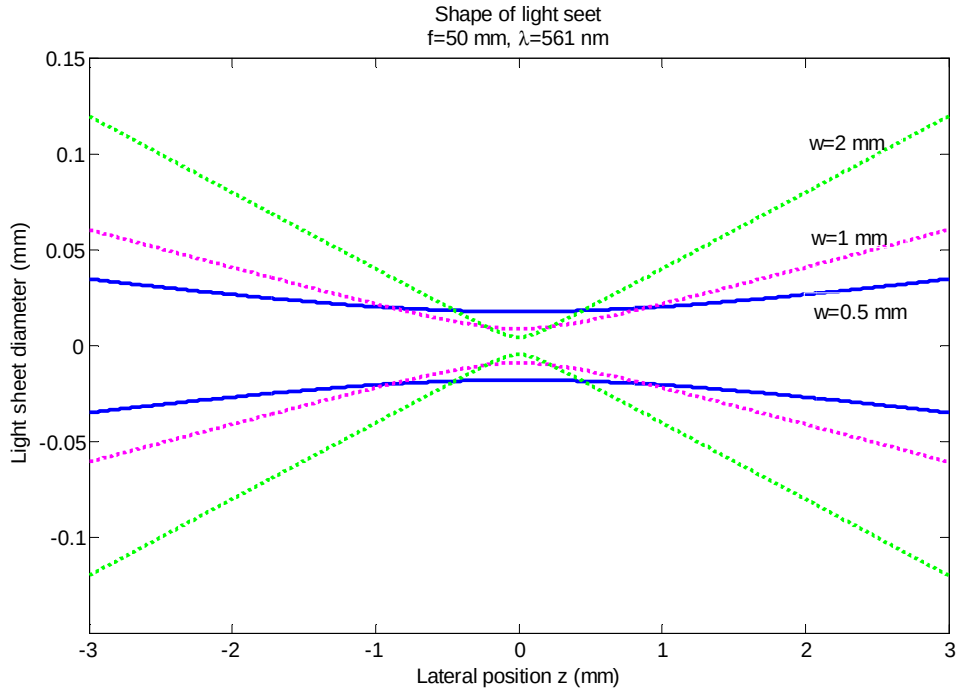

Figure 3. Lateral view of the light sheet.

The lateral resolution of an ultramicroscope is described according to Rayleigh’s criteria:

$$d_{min} = \frac{0.61\lambda}{nNA} \tag{8}$$

Where d_{min} is the minimum distance allowing two points to be resolved, NA is the numerical aperture of the objective and n is the refractive index of the medium, in the clearing solution n_{cl}=1.56. The objective used is a plan apochromatic 10x magnification, NA=0.28, working distance 33.5 mm and focal length equal to 20 mm. This objective was adapted to work in both, air medium and clearing solution medium, by covering it with a cover made of a tube lens and an optical window. Epoxy resin was used to seal this structure avoiding the penetration of oil in the objective. This adaptation can be removed easily to allow both modes of operation. Then d_{min}=0.78 µm when it’s immersed in the clearing solution, and d_{min} =1.2 µm in the air.

The illumination part was aligned with the imaging set by using several targets and micrometers. The main purpose of this process was to centre the beam waist from the cylinder lens in the field of view of the objective, so that focused images can be captured. An important factor is the actual focal length of the cylinder lens that changes by changing the medium. Theoretically, the lens focal in the clearing solution will be:

$$f' = n_{cl} f \tag{9}$$

The CCD camera used was HAMAMATSU C 4742-95-12G04, with 1344(H)x1024(V) pixels. The cell size of every pixel was 6.45x6.45 µm and the effective area 8.67(H)x6.60(V) mm. This is a monochromatic camera which comes with compatible capturing software called HCImage, showed in figure 4.

The sample holder is composed of three stages allowing three-dimension displacements of the sample. Every stage is linked to a motor easily controlled by means of two buttons (forward, backwards). Each motor can be connected to the computer by USB and moved using the motor controller APT, see figure 5.

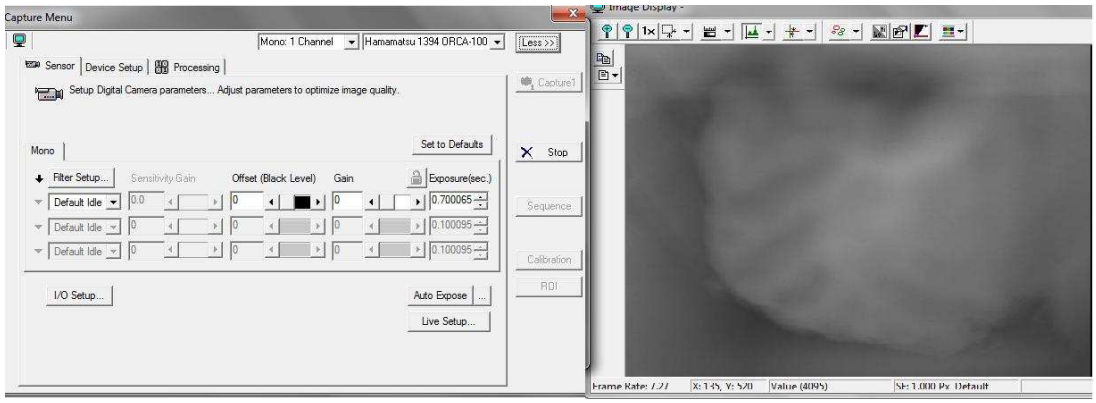

Figure 4. HCImage interface and image display.

Figure 5. APT interface.

2.3. 3D Image Reconstruction

The experimental ultramicroscope presented in this paper captures 2D images that can be post-processed to reconstruct the internal structure of the whole specimen in three dimensions. Although the laser light sheet is fixed, the sample can be laser scanning by moving the stage with the three motor controllers. Therefore, the specimen is scanned from top to bottom generating a stack of 2D images. Then, this stack is recombined by using a Matlab program developed at *Fetal and Perinatal Medicine Research Group (Hospital Clinic-IDIBAPS).* Such software allows a multitask environment to control the scanning process, image capturing and full 3D image reconstruction.

3. Results

All images where captured with the samples immersed in the clearing solution, which presented additional difficulties as it is very corrosive.

Figure 6 shows the first image obtained with the aligned light sheet microscope. It was used a micrometer with a marked dot at the centre (red circle). By using the micrometer was possible to focus and align the illumination and the imaging part.

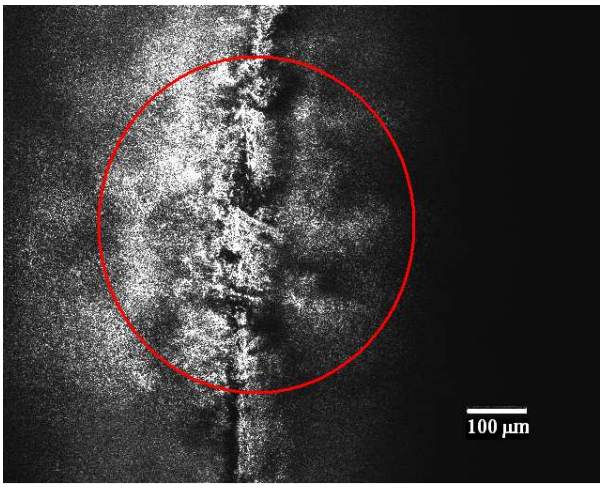

Figure 6. Dot on millimetre paper.

Figure 7 and figure 8 show two different sections of the same rabbit brain, which dimensions are approximately 4x2.5x2 cm. Figure 7 shows a sharper image than figure 8. This is probably because of the distance from the objective.

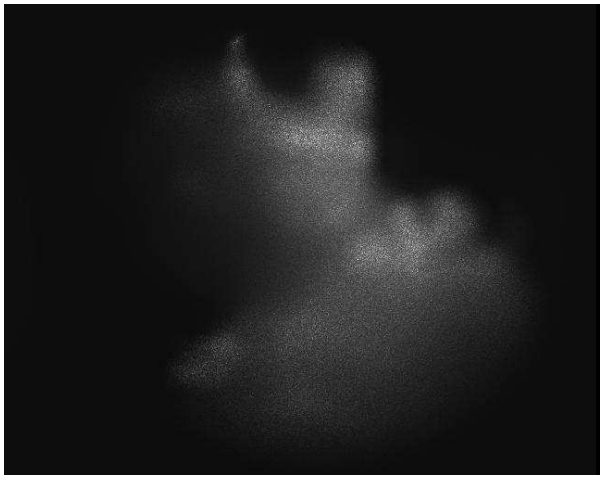
Figure 7. Optical sections of neonatal rabbit, brain’s top.


Figure 8. Optical sections of neonatal rabbit, bottom of the brain.

Also a heart of a rabbit was imaged employing the light sheet microscope. The dimensions of this sample were approximately: 8x5x5 mm. Figure 9 presents the image of the rabbit’s heart when the optical section is, approximately, in the middle of the specimen.

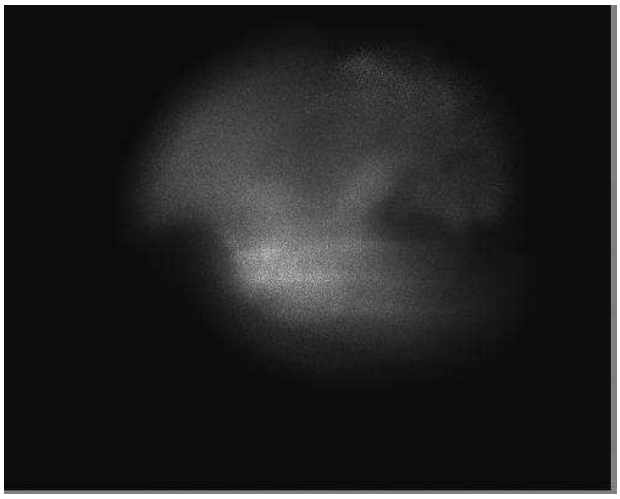

Figure 9. Optical sections of neonatal rabbit’s heart.

In summary, the images presented above show a significant blurring effect. This is due to the thickness of the taken section (18 μm, w=0.5 mm), around 10 cell layers. In histology, the typical thickness is 3-7 μm (less than a cell layer). Then, it is demonstrated the relation between axial resolution and the slit aperture. Although some improvements would enhance the quality of the images, it is obtained a dark field above and below the desired section. These results probe that it is possible to image the internal structures of centimetre-sized specimens by optical sectioning.

4. Discussion

The optimized light sheet microscope allowed the observation of large specimens like rabbit’s brain with sub-millimetre resolution which was the main purpose of this work. The potential resolution could be further increased because, in contrast to conventional confocal microscopy, the illumination and the imaging train were mounted perpendicularly. This can enhance particularly the axial resolution, which is for high NA limited to about three times the lateral resolution. As expected axial resolution greatly depends on the diameter of the slit aperture, see equations (3), (5). Both, the beam waist and the beam width at any point, are inversely proportional to the slit. Thus, in the case of imaging smaller specimens, it is better to use wider slits which provide thinner beam waist as shown in figure 3. In the experiments, the maximum slit diameter employed was 5 mm, which resulted in a high scattering so the results were not valid. The best images were captured with a slit of 1 mm. Although it is desirable to use a smaller slit for larger specimens, it was not possible to cut a slit smaller than 1 mm.

In contrast to other similar techniques, ultramicroscopy accepts low numerical aperture objectives, which provide larger depth of field and better lateral resolution (8). Immersion objectives provide higher NA, thus they yield a better lateral resolution, but on the other side a smaller field of view. At the same time, when an immersion objective is employed the mismatch due to medium discontinuity (difference in the refractive indexes between air and clearing solution) will be improved. To evaluate the feasibility of this option, empirical depth allowed in both cases could be compared.

Comparing to other similar approaches, this ultramicroscope operates by one-side illumination, whereas in the other cases [5] and [8], the use of two-side laser beam to illuminate the whole section at the specimen was preferred as it should provide a higher homogeneity of the illumination. Based on [5] and [8], it is assumed that the sample sizes are similar to the organs used here. Two laser beams may be needed because their samples are not completely translucent, then the light scattering is too high to allow the total propagation through the specimen. Another hypothesis is that the laser feeder provides low power, or that the light sheet dimension is small in comparison with the observed objects. These three drawbacks do not appear in this ultramicroscope, since it was optimized to handle centimetre-sized specimens.

After the clearing process all the samples were completely transparent (see figure 1), it was difficult to find them in the clearing solution. The laser beam went through them easily as seen in figure 2, where an invisible brain was placed in the path of the beam, inside the chamber. Furthermore, the laser power was adjusted by using several attenuators (the equivalent attenuation is 3 dB) because it was observed that the laser beam burns the sample in long-term exposures, causing the bleaching of the specimen. The time to bleach a transparent specimen is inversely proportional to the power of the beam.

Related to the light sheet, a cylindrical lens of 5 cm length was selected to obtain a light sheet wide enough to illuminate the whole specimen on each optical section. The focal length of this lens was 50 mm, but this value changes in the clearing solution. In this case, the theoretical focal length (9) is f_{theor}'= 78 mm, although experimentally a result of $f_{experim}$'= 73 mm was obtained. This difference was expected because the beam goes first through the air and then, after some distance (not fixed), penetrates in the chamber. Thus, the cylindrical lens was mounted in a translation stage to move it as required, depending on the position of the chamber. So that, for every sample observed, this lens was horizontally aligned to be on focus. This phenomenon of misalignment, regarding the objective, can be observed in figure 10 where the focus should be moved forward.

The focal length of the objective also changes when it’s immersed in the clearing solution. In such case, there isn’t any change of the medium and f'=3.12 mm, instead of 20 mm as in air.
Concerning the image quality, although this experiment probes that optical sectioning is possible, as expected, the detail of the images obtained could be enhanced.

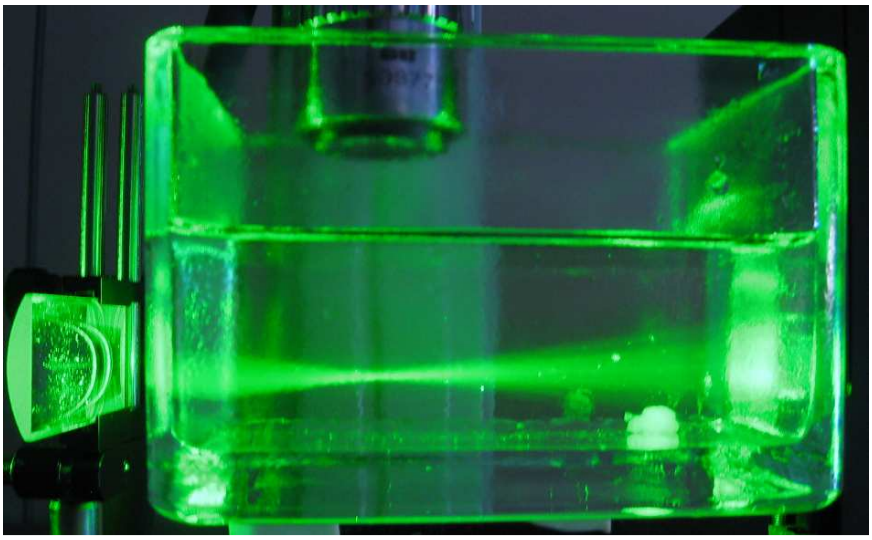

Figure 10. Example of light sheet for a slit aperture diameter of 10 mm.

A reliable technique to remove the blurring effect (observed in figures 6-9), and provide more detailed images, is: fluorescence. In most cases, a component of interest in the specimen can be labelled specifically with a fluorescent molecule called a fluorophore (such as green fluorescent protein (GFP), fluorescein or DyLight 488). The specimen is illuminated with light of a specific wavelength range which is absorbed by the fluorophores, causing them to emit light of longer wavelengths. Each fluorophore is characterized by the excitation and emission wavelengths. The illumination light is separated from the much weaker emitted fluorescence through the use of a spectral emission filter placed after the objective. The filter is chosen to match the spectral excitation and emission characteristics of the fluorophore used to label the specimen. Thus, the distribution of a single fluorophore is imaged at a time. Also, it is important to check the spectral response of the CCD camera (QE versus wavelength). The camera used in this setup provides high sensitivity along the entire visible spectrum.

In the future, ultramicroscopy could serve as a powerful tool for research imaging in a wide range of applications in life sciences. At *Fetal and Perinatal Medicine Research Group* (IDIBAPS) they are interested in using the ultramicroscope to investigate Fetal Growth Restriction (FGR) which affects 4% of the Spanish population at a significant level. The main consequences of FGR are motor and neurological disabilities, strongly related to the abnormal development of the frontal part of the brain, where the cognitive functions are managed. Therefore, it will be very useful to image the neuronal networks. Studying the fetal formation of affected brains, this research group could investigate the specific diseases derived. Neurons could be observed using the ultramicroscope combined with fluorescence by applying immunohistochemical labelling through secondary fluorescent antibodies found specifically in neurons [8]. Also, the heart is a key element to study this condition, so this organ could be imaged by labelling specific blood molecules with fluorophores, to analyze the development of blood circuits (vessels and arteries distribution).

5. Conclusion

This exploratory study regarding the impact of the aperture slit on axial resolution of 3D images and how even a fundamental diffraction principle is enough to obtain result for life sciences with a potential high impact in life sciences.

Comparing light sheet microscopy to other state-of-the-art technologies, as standard confocal or 2-photon microscopy, low NA objectives can be used. This setup offers high resolution 3D images at deep layers of tissue even using single photon phenomena and post-processing and correct acquisition provides full 3D reconstructions of juvenile rabbit’s brain.

Furthermore, it was shown that the diameter of the slit aperture was crucial in the axial resolution of the design.

In conclusion, although ultramicroscopy applied to transparent specimens is in its first phase, the results show that this is a promising technique that in the near future could fill a gap between different available imaging techniques to help solve new biological questions.

Acknowledgments

This research was developed in the *Fetal and Perinatal Medicine Research Group* (IDIBAPS). I am indebted to my advisor Ivan Amat-Roldan and the members of IDIBAPS, for their help and encouragement throughout the course of this work. Also, I greatly appreciate the collaboration of Prof. David Artigas as my tutor.

References

[1] Gonzalez R, Woods R 2006 *Digital image processing* (New York: Addison-Wesley Publishing Company)
[2] Frankel F 2002 Envisioning science: the design and craft of the science image *The Massachussets Institute of Technology Press* (192-245)
[3] Zsigmondy R 1926 Properties of colloids, *Nobel Prize Lecture*
[4] Rylander C, Stumpp O, Mendenhall J and Diller K Dehydration mechanism of optical clearing in tissue *Journal of Biomedical Optics* Vol. **11** (4) 041117 (1-7)
[5] Becker K, Jährling N, Kramer E, Schnorrer F, Dodt U 2008 Ultramicroscopy: 3D reconstruction of large microscopical specimens *Journal of Biophotonics* **1**, No. 1 36-42
[6] Zajaz H 1986 Optics (Delaware, Addison-Wesley) (106-185)
[7] Silfvast W 1996 Laser fundamentals, (Cambridge, Cambridge University Press) (399-439)
[8] Dodt U, Leischner U, Schierloh A, Jährling N, Mauch P, Deininger K, Deussing J, Eder M, Zieglgänsberger, Becker K 2007 Ultramicroscopy: three dimensional visualization of neuronal networks in the whole mouse brain *Nature Methods* Vol. **4** No. 4 (331-336)